The details of studies carried out under my supervision for the Sun Pharma Science Foundation Research Award, 2023

The details I have illustrated below are the various studies and the experimental results obtained for the past 3 decades, that is documented here for the ***Sun Pharma Science Foundation Research Award, 2023.*** The details are categorised into 4 different groups. None of them are presented anywhere for any award:

A. Identification and synthesis of molecule that specifically interacts with Hcy in presence of other animo acids in biological fluids.

B. Aptamers for the specific interaction and identification of Hepatitis C antigen.

C. Development of mRNA based vaccine platform for COVID-19 and other infectious diseases.

D. Synthesis of anti-cancer molecules and biological characterization by biophysical and biochemical assays.

A. Identification and synthesis of molecule that specifically interacts with Hcy in presence of other animo acids in biological fluids.

In this part of the study, we have attempted to synthesise a copper complex that specifically interact with Homocysteine (Hcy). Homocysteine is well known as an independent risk factor for the identification of atherosclerosis (thickening or hardening of the arteries). Arteriosclerosis is also known for continuous inflammatory damage to the arterial intima with increased permeability to plasma, deposition of plasma lipids in plaques and fibrosis and calcification of plaques. The correlation between hyperhomocysteinemia (it is referred as a condition where greater than 15 micromol/L of homocysteine is found in the blood) and atherosclerotic disease was first proposed more than 40 years ago. Atherosclerosis is the most common pathological process that leads to cardiovascular diseases such as myocardial infarction (MI), heart failure, stroke and claudication.

To address this issue and to identify the estimation of Hcy in human plasma, a series of copper(II) compounds 1–4 were synthesized and developed as fluorogenic probes to measure the cardiac marker homocysteine (Hcy) without any interference from other bioanalytes prevalent in human blood plasma including, cysteine and glutathione. UV-vis and EPR studies have provided confirmatory evidence for reduction-induced-emission-enhancement of the probe, which is responsible for the observed ‘‘off-to-on’’ behaviour towards Hcy. Water solubility, remarkable fluorescence enhancement (55–111 fold), and low detection ability (nearly 2.5 lM) make the probe suitable for clinical testing of cardiac samples. Investigation of 1 against a few reductive interferents testifies its specificity for Hcy. Results from clinical examination of cardiac samples by 1 when combined with the outcome of the reliability testing involving a clinically approved commercial immunoassay kit, validates the prospect of the molecular probe for direct measurement of Hcy in human plasma, which is unprecedented. The following diagram (figure 1) shows the structure of the synthetic molecule and its specific interaction with Hcy compared to other amino acids.

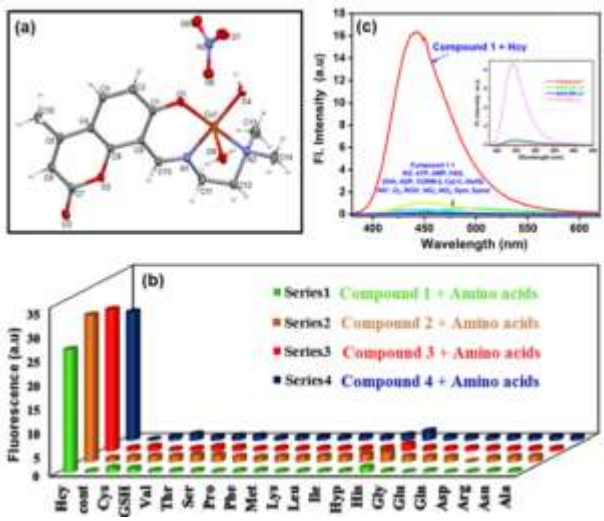

Figure 1. **a.** ORTEP view and atom numbering scheme of the copper compound used in the study. **b**. Bar graph showing the specific interaction of the synthetic molecule with Hcy in presence of other amino acids. **c.** Fluorescence enhancement of Hcy in presence of 20µM concentration of synthetic compound in presence of other biologically relevant species (125 µM). In the inset, fluorescence of 20µM concentration of synthetic compound in presence of variable concentrations of NaHS is shown.

To quantitate Hcy in different samples and also in human plasma, a standard curve is prepared as shown below (figure 2). Fluorescence of Hcy is recorded at 439 nm. Using this standard curve only quantification of Hcy in different human plasma samples was done.

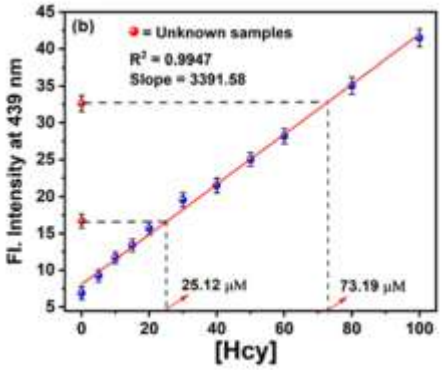

Figure 2. Fluorescence intensity of Hcy at 439 nm on exciting different concentrations of Hcy.

Similarly, the absorbance of Hcy in the presence and absence of synthetic molecule is recorded as shown below. The electronic spectrum of synthetic compound alone (Fig. 3) displays a d–d band at 625 nm. But upon addition of Hcy, the band disappeared suggesting the formation of Cu(I) species. The details are shown in figure 3.

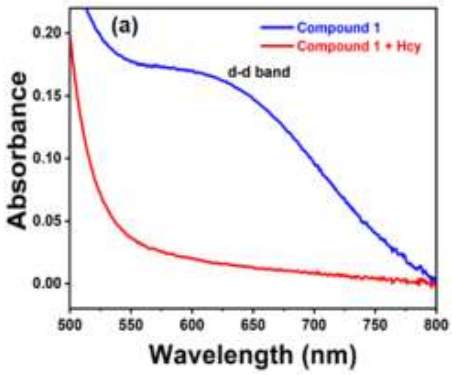

Figure 3. Absorbance of synthetic small molecule in the presence and absence of Hcy.

Clinical validation of the synthetic compound was done by considering blood samples from 56 human beings (19 healthy and 37 cardiac patient samples) and plasma was extracted from the samples. Assay details were shown in the figure 4.

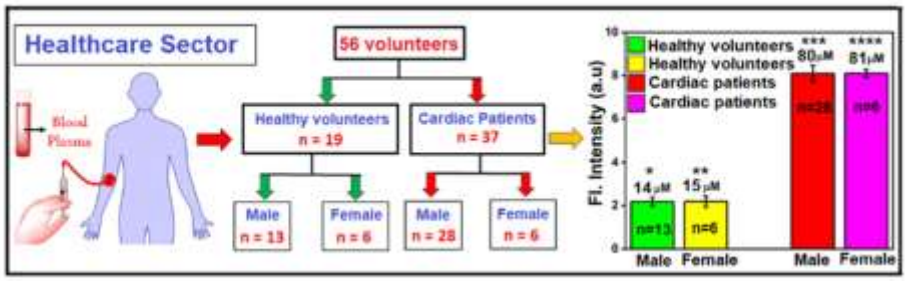

Figure 4. Schematic representation of Hcy measured in both healthy and cardiac patient samples and the results obtained in the clinical validation.

This part of the study was published in Chem Comm., the details of the publication is given below:

A unique water soluble probe for measuring the cardiac marker homocysteine and its clinical validation.(2022) Snehasish Debnath,Ratish R. Nair,Riya Ghosh, Gaddam Kiranmai,Narsini Radhakishan, Narayana Nagesh* and Pabitra B. Chatterjee*. *Chem Comm.*, 58, 9210 - 9213. (IF-5.0)

B. Aptamers for the specific interaction and identification of Hepatitis C antigen.

An attempt was made to develop a prototype dot blot device for the detection of Hepatitis C viral protein that forms complex with AuNP-aptamer on paper. Specific aptamers that form unique folded structures and interact specifically with Hepatitis C viral (HCV) antigen was identified and synthesised. Later one end of the aptamer is aminolated and tagged with AuNP. The aptamer with AuNP at one end is hybridized to the surface of a special paper using chemical methods. Aptamer immobilization strategy by using a linker molecule has been successfully carried out and tested.

Chemistry of linker between paper and aptamer has been characterized by FT-IR and fluorescence experiments have been performed.

7 aptamers were selected for the core HCV protein interaction. It was found that out of 7 three aptamers have given good result. The single stranded DNA aptamers that were raised through SELEX process and shown to be specifically binding and inhibiting HCV core antigen are used. The aptamers are listed in the table below.

1	**C new**	**AGTGATGGTTGTTATCTGGCCTCAGAGGTTCTCGGGTGTGGTCA**
2	**C4**	**GCACGCCAGACCAGCCGTCCTCTCTTCATCCGAGCCTTCACCGAGC**
3	**C7**	**ACTATACACAAAAATAACACGACCGACGAAAAAACACAACC**
4	**C42**	**CATATCAGACACAACACAACAAAACACATACATACAACGCC**
5	**C97**	**TAACACACACAACTTAAAATCATACAAAAAAGAGTAAATGC**
6	**C103**	**TACCACACATGCAGACCCACACAAATACATACTAGAGACAC**
7	**C104**	**CCAAATACTACCGCAAAAACCACCTCCCCCTCGATAATAGC**

The possible folded pattens of C7 and C97 aptamers are shown below (figure 1)

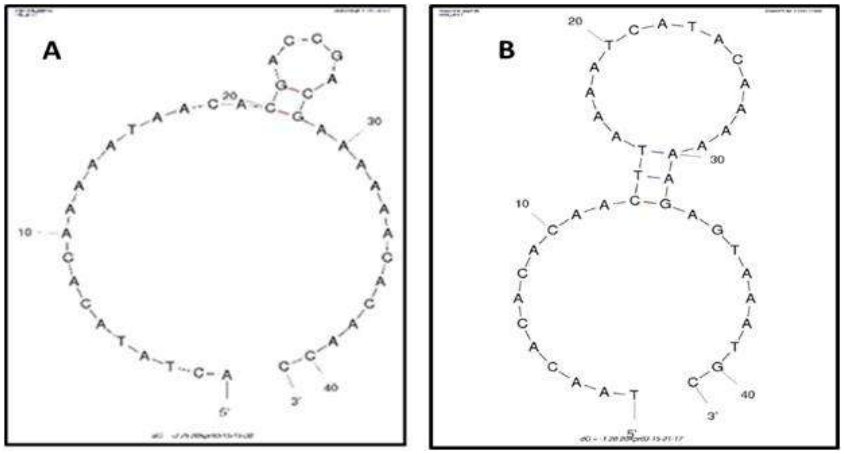

Figure 1: Images of predicted secondary structures of aptamers from Mfold.
A: Predicted secondary structure for C7 B: Predicted secondary structure for C97

Functionalization of paper to achieve aptamer binding modification of cellulose surface with Amino Xyloglucan (NH_2-XG) and Phenylene diisothiocyanate (PDITC)

The schematic process used for modification of paper surface for immobilization of aminolated aptamer is shown in figure 2. The modification of paper was characterized by FTIR, UV, fluorescence, Ninhydrin test and Scanning Electron Microscopy. Some of the important results are shown here.

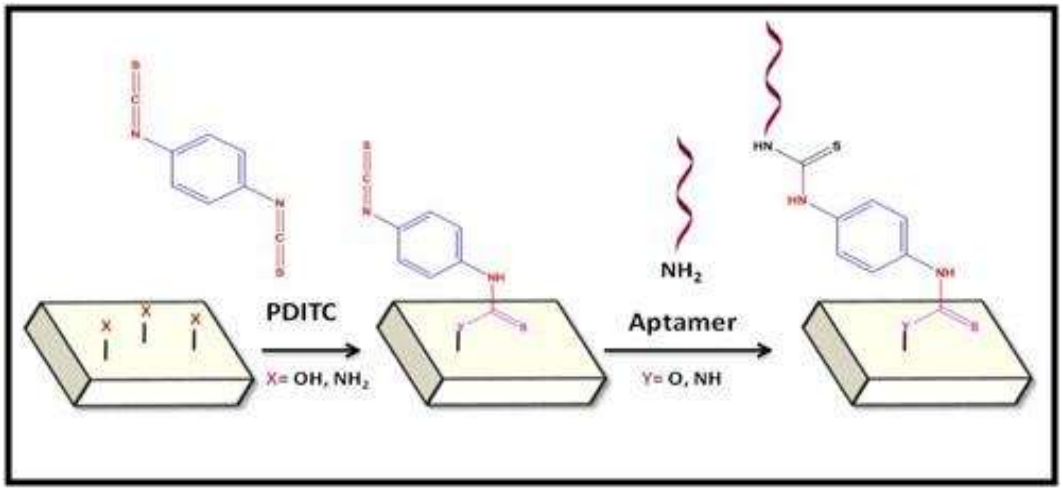

Figure 2. Schematic representation of a modification of cellulose surface for aptamer binding.

For immobilization of the aptamer the paper surface is modified with amino xyloglucan and tested under the UV light. The Unmodified paper does not show any fluorescence (Figure 3 A) where as (Figure 3 B) xyloglucan modified paper exhibits greenish blue colour fluorescence, due to the presence of amino group. The paper fluorescence gets reduced due to the attachment of Phenylene diisothiocyanate (PDITC - a linker for tagging the aminolated aptamer) (Figure 3C). The blue fluorescence colour in the (Figure 3 D) is due to the hybridization of aminolated apater and excess unbound aminolated aptamers, sitting on the paper surface. The excess of aptamers get washed off after washing with buffer.

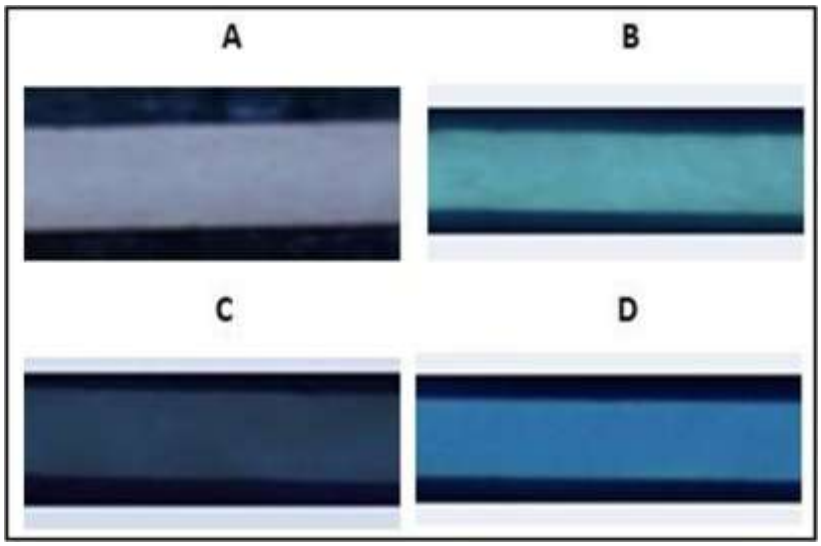

Figure 3. Images of papers under UV light after each step of paper surface modification.
A: Unmodified paper: B: Paper modified with NH_2-XG; C: Paper modified with NH_2-XG and PDITC; D: Paper modified with NH_2-XG and PDITC bound to aptamer C7.

As a confirmatory test for the presence of amino group on the surface of paper, Ninhydrin test was carried out (Figure 4). It is a common test for the presence of primary amine group. The test shows the brown colour development when the amino group of free amino acid reacts with ninhydrin (Figure 4 B). When the paper is modified with NH_2-XG, PDTIC and NH_2-C7; exposure or masking of amino groups results in no or very light brownish yellow colour on the surface of the paper as shown in the figure 4C and 4D.

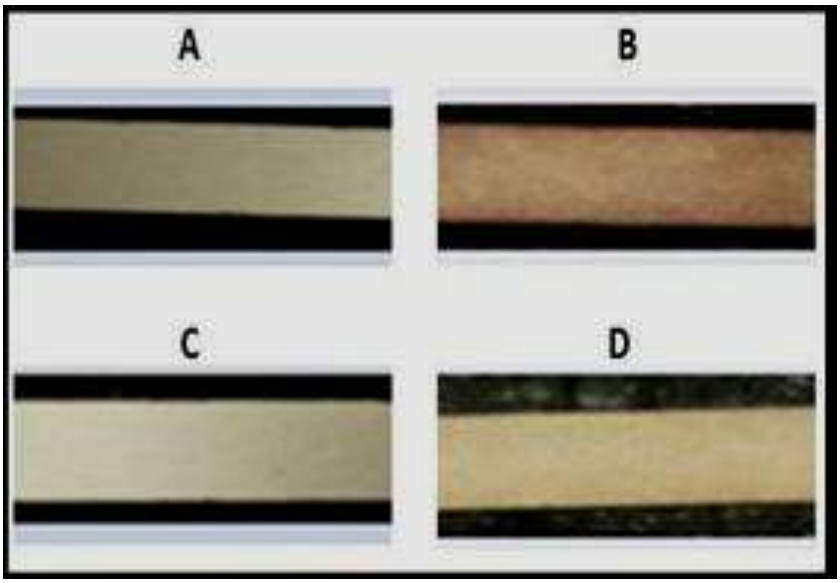

Figure 4. Images of paper to ninhydrin test after each step of modification. A: Unmodified paper; B: Paper modified with NH_2-XG; C: Paper modified with NH_2-XG and PDITC; D: Paper modified with NH_2-XG and PDITC bound to aptamer.

Cellulose fibres of the paper strip should be intact after the surface modifications because the lateral movement of the liquid occurs through the cellulose fibres. The voids between the cellulose fibers should not be blocked by the chemical used to modify the surface of the cellulose. The flow of the liquid should happen through the capillaries of the paper and hence it should be free. SEM images (Figure 5) of the paper strips were taken to obtain the surface topography and to visualize the cellulose fibers. The main objective of taking SEM images after each step of modification was to determine the effect of these modifications on cellulose fibers in the paper.

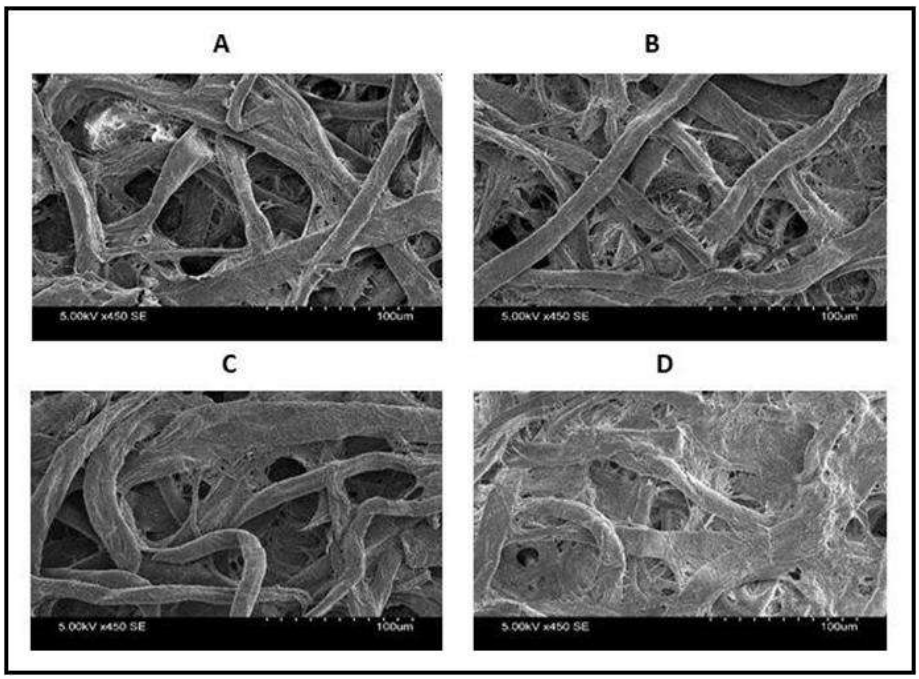

Figure 5. SEM images of paper after each step of modification. A: Unmodified paper; B: Paper modified with NH_2-XG;C: Paper modified with NH_2-XG and PDITC; D: Paper modified with NH_2-XG and PDITC bound to aptamer

Surfactant free low pH based conjugation of aptamers with gold nanoparticles:

The conjugation of GNPs with aptamer was achieved successfully and was characterized by UV-vis Spectrophotometry, Dynamic light scattering (DLS), Zeta potential and Transmission Electron Microscopy.

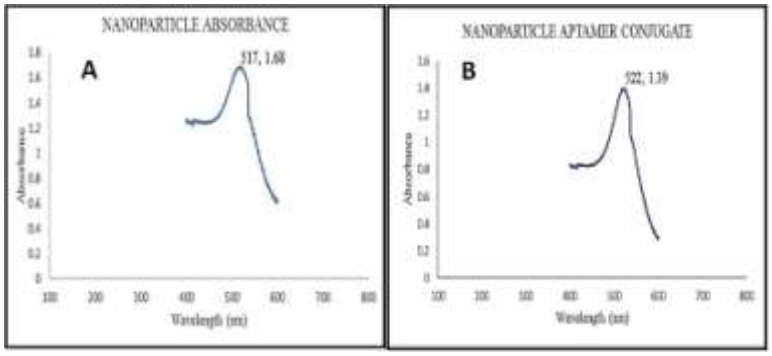

Figure 6. UV visible spectra of gold nanoparticles: A: AuNP before conjugation with aptamer. Λmax = 517nm; B: AuNP after conjugation with aptamer λmax = 522nm.

AuNPs shows an absorbance peak in the visible region (500nm-600nm) due to an optical feature commonly referred to as localized surface plasmon resonance (LSPR). LSPR is the collective oscillation of electrons in the conduction band of gold nanoparticles in resonance with a specific wavelength of the incident light. Based on the difference in the size and shape of gold nanoparticles, the LSPR spectrum also varies which shows as absorption maxima on UV-vis spectrophotometer. A shift in the peak of absorption maxima by from 517nm to 522nm infers the adsorption of aptamers on AuNPs

DLS is used to measure the hydrodynamic size of the sub-micron sized particles. The hydrodynamic size of a particle includes the surface coating and the solvent layer that is associated with the particle and hence it is more useful in identifying the modifications on the particle surface. With the help of DLS, particle size and characterizing the modification of the nanoparticles can be performed.

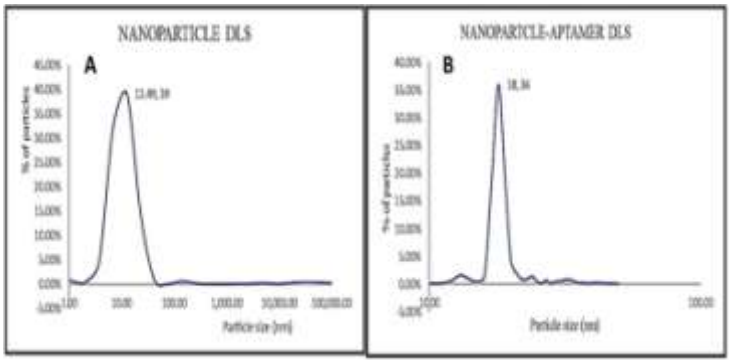

Figure 7. Hydrodynamic sizes of gold nanoparticles. A: AuNP before conjugation with aptamer = 12.49nm;B: AuNP after conjugation with aptamer= 18nm.

An increase in mean hydrodynamic radius of AUNPs can be an evidence for aptamer adsorption on AuNPs.

After the conjugation of aptamer the change in the zeta potential from -37 mV to -13.6 mV, which might be related with the presence of the negatively-charged aptamer at the nanoparticle surface.

Figure 8. Zeta potential of gold nanoparticles: A:AuNP before conjugation with aptamer = -37mV; B: AuNP after conjugation with aptamer= -13.6mV

TEM images can be taken to determine the physical particle size and the structural morphology of the gold nanoparticles. TEM images can also help in visualizing the particle distribution and counting the number of isolated particles (Figure 9 A). Increase in size and a brighter periphery of

around the nanoparticle was observed after conjugation. Also, the average size of the AuNPs increased from 10.5nm to 13.8nm which van be attributed to adhereing of aptamers on AuNPs (Figure 9 B).

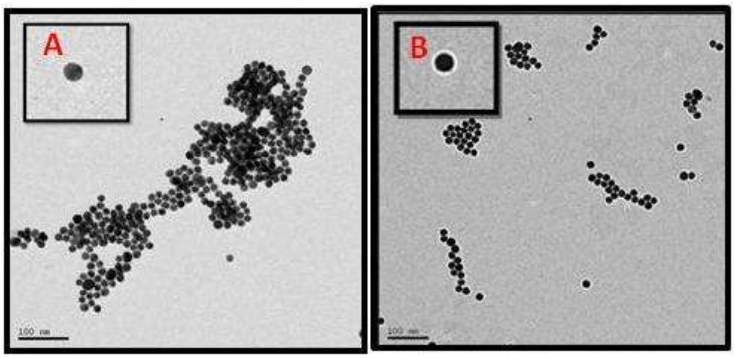

Figure 9: Transmission Electron Micrographs of gold nanoparticles: A: AuNP before conjugation with aptamer= 10.5nm; B: AuNPs after conjugation with aptamer = 13.8nm.

Design for Dot Blot device prototype:

In order to establish the proof of concept of detection on paper device, all standardization and validation studies were done on prototype Dot Blot devices. These are easier to handle as all reaction components are added at a spot on the paper and thus interactions are verified.

The parts of a Dot Blot device:

1. Dot Blot Test strip: AXG PDITC modified G4 Whatman® Grade-4 paper was taken for this purpose.
2. Absorption pad: Made of cellulose. Its primary function is to wick the fluid through the membrane.
3. Backing membrane: This is an adhesive strip onto which the entire device can be attached. It holds the device in position for.

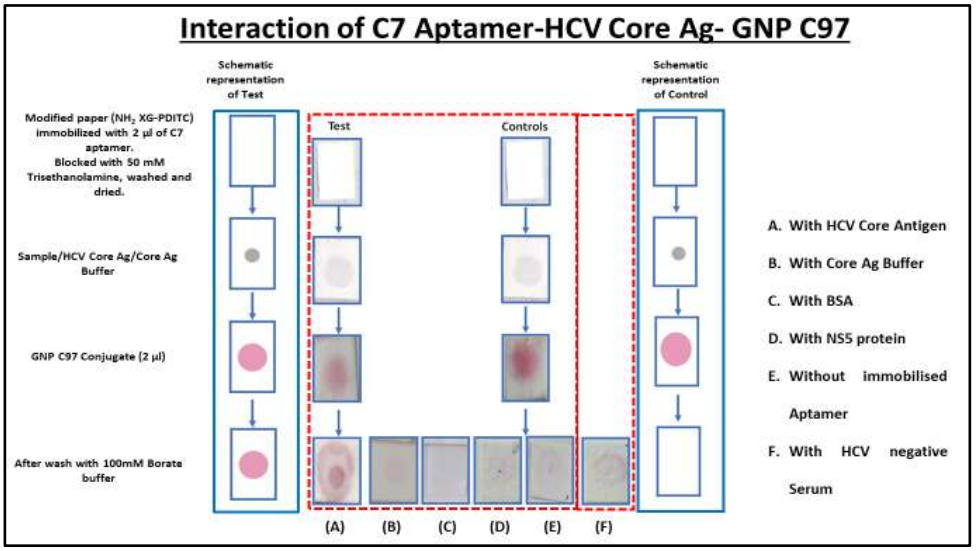

Figure 10: Operational Flowchart of the Dot-Blot-Device prototype and result with appropriate results.

The results obtained in this study are yet to be published in a reputed international journal .

C. Development of mRNA based vaccine platform for COVID-19 and other infectious diseases.

To control the COVID-19 infection CSIR has asked CSIR-CCMB and 5 other CSIR labs (working on different fields of science) to work together and develop a mRNA vaccine platform to (more or less a replica of Moderna mRNA vaccine) combat COVID-19 in our country. I am the nodal PI for this project (mRNA Platforms for Vaccine and Therapeutics) and we have achieved the following in the span of around 18 months.

• Design and generation of an in vitro transcription DNA template(s) encoding spike protein of SARS-CoV2 along with the properties that enhances the *in vivo* translational efficiencies of the *in vitro* transcribed mRNA. The mRNA would be optimized for stability and immune avoidance using experimental and bioinformatics tools.

• Optimization of *in vitro* transcription platform using the customized DNA template that include modified nucleosides, rNTPs, various polymerases etc.

• Optimization of lipid: mRNA complexation and characterization of resulting particles.

• Assessment of the protein expression of spike in cell lines and in small animals and confirmation by immunological method and also assessment of immune response using various immune markers.

The various experimental details to generate mRNA vaccine for COVID-19 is shown below:

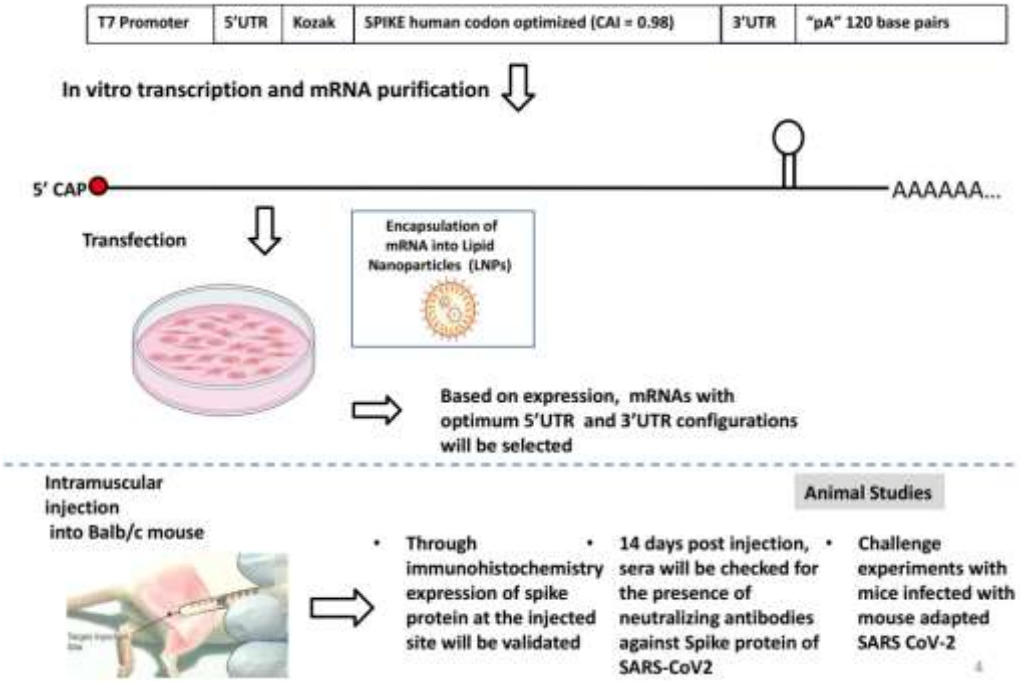

The various steps we followed to generate mRNA vaccine at CCMB

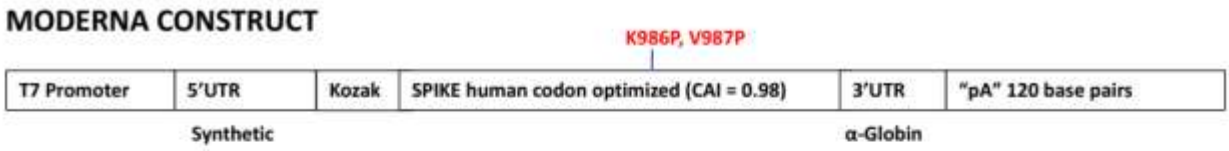

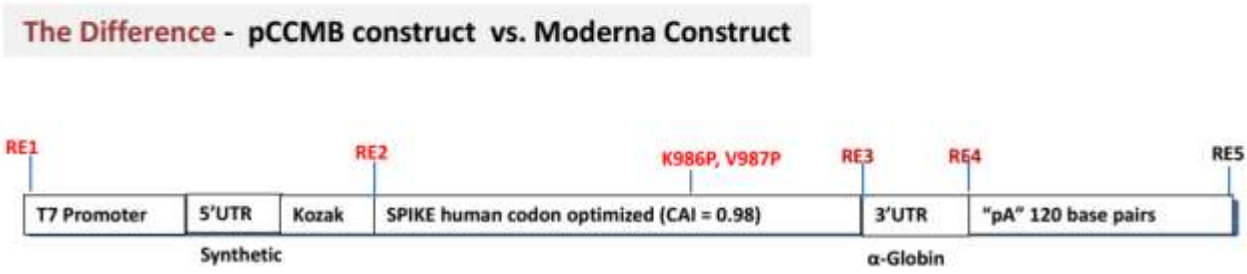

The construct developed at CCMB, keeping Moderna construct as the base.

The expression of spike protein in with pseudouridine in HEK293T cells is shown below.

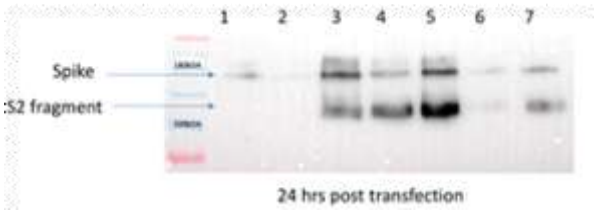

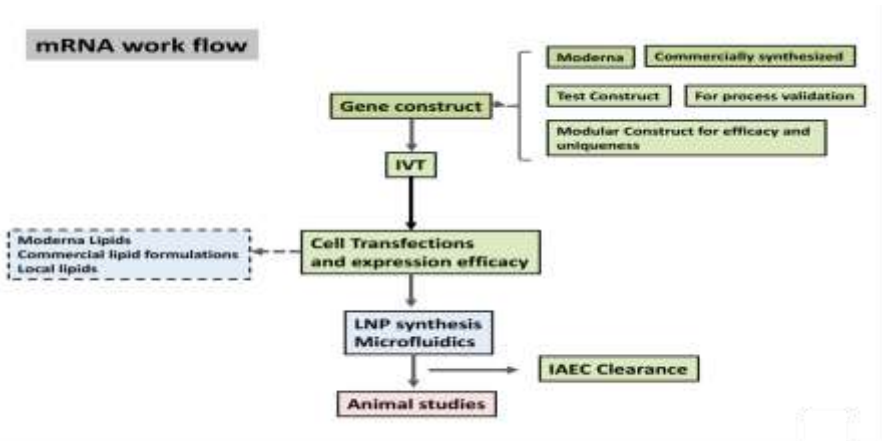

After the expression of spike protein the lipid encapsulation is done using the lipids designed by us as well as the lipids commercially procured ones. The lipid encapsulated forms were first tested in cell lines and later they were assayed using animal models (both mouse and hamster models). The final results indicate shows that the mRNA vaccine prepared at CCMB is showing good results.

Now efforts are in progress to study the efficiency of the mRNA vaccine platform for the other infectious diseases.

D. Synthesis of anti-cancer molecules and biological characterization by biophysical and biochemical assays.

Several small molecules were synthesised and studied in my laboratory at CCMB for the past 3 decades on their efficiency to server as anti-cancer molecules. Few molecules like AZT, indole derivatives, β-carboline derivatives etc., were shown to exhibit anticancer activity. Here, I have chosen couple of β-carboline derivatives and documented how their role as anti-cancer molecules was extensively studied in my lab.

The β-carboline molecules are the alkaloids found in nature. The β-carboline alkaloids are the interesting class of molecules with a wide variety of medicinal properties including anticancer activity. Small molecules with β-carboline scaffold such as Harman, Harmine, Norharman and Harmaline are isolated from *Peganum harmala* (Zygophillaceae, Syrian Rue). The β-carboline scaffolds contain a tricyclic planner structure that is capable of intercalating with DNA and inhibit topoisomearse effectively. The anticancer activities of these molecules are known to be due to interaction with DNA either through intercalation or through external binding, topoisomerase inhibition, kinesin spindle protein (KSP) inhibition etc., however, in cancer therapy, the DNA intercalative topoisomerase inhibition has attained significant importance in cancer therapy. The anticancer activity of several synthetic compounds displays these mechanisms of action.

Hence, in several of our studies where modified β-carboline molecules were used are assayed for both topo I and topo II inhibition activity. Since, the molecule's interaction with double stranded and topoisomerase inhibition are considered as a crucial, few podophyllotoxin linked β-carboline and β-carboline-bisindole congeners were synthesised and assayed for its potential to interact with DNA and inhibit topoisoemerase using biophysical and biochemical approaches.

Broadly, the topoisomerases are classified into two of types, topo-I and topo-II. Since topo-I It is involved in replication and proliferation process, over production of topo I was noticed in cancer cells compared to normal cells. In general, topo I controls the changes in the DNA structure by cutting a single stranded DNA and re-joining the phosphate backbone during the normal cell cycle. Mechanism of topo I inhibition is known to occur in two ways, these inhibitors may bind topoisomerase directly or they may bind to DNA and alter its structure, so that it cannot be recognized by topoisomerases. The assay showing the inhibition of topo- I by few synthetic β-carboline- bisindole compounds tested by us are shown below in figure 1.

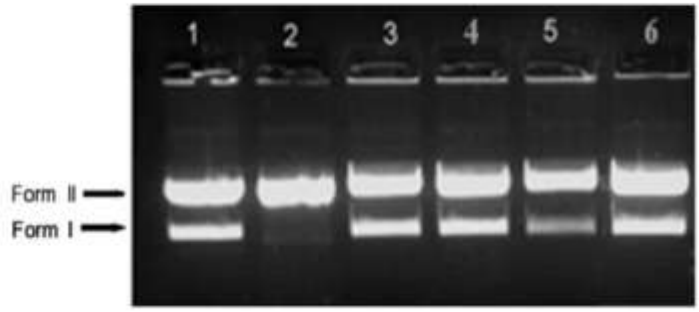

Figure 1: Agarose gel picture showing the inhibition of topo I by β-carboline- bisindole compounds. Lane1- pBR322 along; Lane2- pBR322 with topo I; Lane3,4 and 5- with different β-carboline- bisindole compounds; Lane6- pBR322+topoI +Camptothecin.

Where as, topoisomerase II is a nuclear enzyme that controls the DNA structure by catalysing the DNA cleavage and re-ligating the phosphodiester bonds. Recently, topoisomerase II inhibitors have gained importance as most of them interfere with the re-ligation process. The effect of synthetic β-carboline compounds on topoisomerase II inhibition was assayed by treating the mixture containing of synthetic compounds and topoisomerase II with kinetoplastid DNA (kDNA). kDNA is a form of macromolecular DNA structure in which several circular DN A structures are catenated to each other to form a network of interlocked rings.

When kDNA is incubated different concentrations of β-carboline molecules that inhibit topo II activity, and subjected to electrophoresis, relatively fast migrating bands were observed, indicating the complete conversion of catenated DNA form to decatenated forms like nicked circular, linear and relaxed forms. If the DNA is not cut by the enzyme, the bands corresponding to relaxed DNA will not be seen. However, most of kDNA remained as catenated form and remain near the wells. Since catenated kDNA is highly supercoiled, it remains in the well without entering the gel. There are two varieties of topo II inhibitors like ITD and IFP. The observational results obtained from our studies indicate that couple of synthetic β-carboline molecules (namely 7i and 7j) Catalytic Inhibitory Compound or CIC. The results obtained from various synthetic β-carboline molecules used in our study are shown below (figure 2)

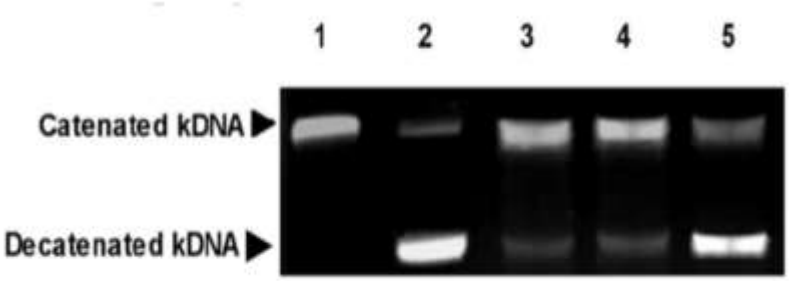

Figure 2: Agarose gel picture showing the inhibition of topo II by podophyllotoxin linked β-carboline compounds. Lane1- Catenated kDNA alone; Lane2- Catenated kDNA with topo II (5 units); Lane 3 and 4 - kDNA+ 5 units of topo II with different β-carbolinepodophyllotoxin compounds; Lane6- kDNA+ 5 units of topoII +Etoposide.

The β-carboline- bisindole compounds were found to break DNA by generating free radicals. To study the effect of UV-light on the extent of DNA photocleavage by the free radicals generated by β-carboline- bisindole compounds, was studied in the presence and absence of UV-light. In the presence of UV-light (first gel picture) the β-carboline- bisindole compound generate more of free radicals and cleave supercoiled plasmid DNA (pBR322) (form I) to relaxed form of DNA (form II) where as in the absence of UV-light (in dark, second gel picture) the effect of β-carboline-bisindole compounds on supercoiled pBR322 plasmid DNA is not seen (the band intensity of pBR322 remained same throughout, indicating less or no effect of free radicals in the absence of UV light). These results indicate that β-carbolinebisindole compounds are suitable for photodynamic therapy (PDT). The results are shown in the gel below (figure 3)

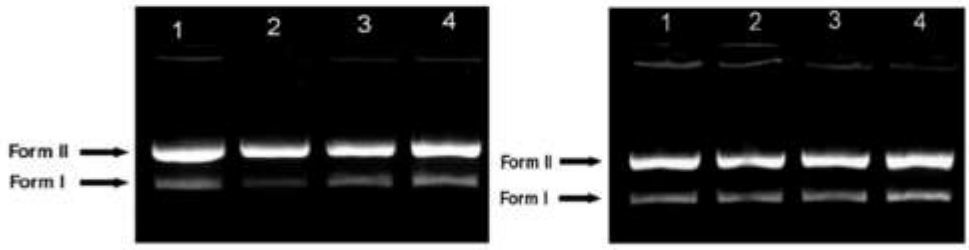

Figure 3: Gel electrophoresis picture showing the photo cleavage of pBR322 DNA by β-carboline -bisindole compounds in the presence and absence of UV light.

The role of β-carboline scaffolds synthesised and assayed in our laboratory indicate that they have very good binding interaction with double stranded DNA. In most of the cases, they will intercalate with dsDNA and few cases, they may show combilexin type of interaction with DNA (i.e both intercalation and external binding). Since most of the cell biological studies are linked to DNA, the information on the nature of β-carboline scaffolds interaction with dsDNA will through light on the manner in which β-carboline scaffolds interact with DNA and exhibit anti-cancer activity. DNA binding studies are done using spectroscopic techniques like, UV-vis, Fluorescence, and Circular dichroism and Viscosity studies. Molecular modelling studies were carried out to understand the nature of small molecular interaction with macromolecules. The data spectroscopy data collected using β- carbolinebisindole compounds (**7g** and **7r**) is shown below. The data indicates that these molecules have combilexin type interactions with dsDNA. The various spectra obtained from biophysical experiments are shown below (figure 4)

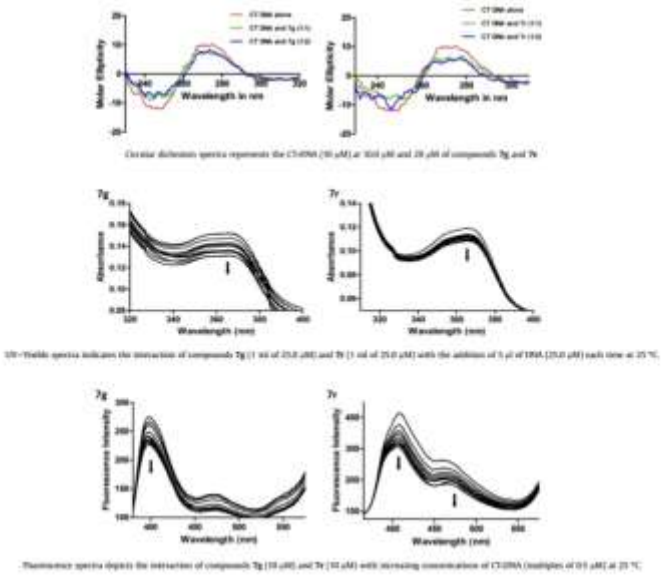

Figure 4: β-carbolinebisindole compounds (**7g** and **7r**) interaction with dsDNA (CT-DNA).

Cell biology studies include MTT, comet, cell cycle and apoptosis assays. With β-carboline -bisindole and Podophyllotoxin linked β-carboline compounds, it was identified that they inhibit Topo I and Topo II enzymes. Both the compounds inhibit cancer cell growth much effectively compared to normal cells. Cell cycle assay indicate that both type of β-carboline compounds studied were inhibiting the cell cycle at G2/M phase in cancer cells compared to normal cells. Both varieties of β-carboline compounds induce apoptosis among cancer cells. With

Podophyllotoxin linked β-carboline compounds, comet assay was performed to assess the extent of DNA damage occurred with the addition of Podophyllotoxin linked β-carboline compounds. Double-strand DNA in DU-145 cells was cleaved by Podophyllotoxin linked β- carboline compounds similar to the control, Etoposide. In the present assay Propidium Iodide, a fluorescent DNA-binding molecule was used to detect the extent of DNA damage. DU- 145cells were treated with 10μM of Podophyllotoxin linked β-carboline compounds and Etoposide, and after lysis the samples were allowed to undergo electrophoresis. Cells grown in the absence of any congeners is considered as control. It was observed that the DNA damage is taking place in presence of Podophyllotoxin linked β-carboline compounds and Etoposide (details were shown in figure 5). However, there is no DNA damage observed in the control. Etoposide is well known topoisomerase II inhibitor which exhibits this inhibition activity through stabilizing the DNA cleavable complex. It was known earlier that Etoposide will induce the formation of open circular and linear DNA through the topoisomerase-DNA cleavable complex formation. We speculate that Podophyllotoxin linked β-carboline compounds may also effectively damage the DNA like Etoposide and inhibit the activity of topoisomerase II. The results obtained indicate that Podophyllotoxin linked β-carboline compounds are having potential to damage the cellular DNA effectively and stop the growth of cancer cells. The effect was found to be less with normal cells.

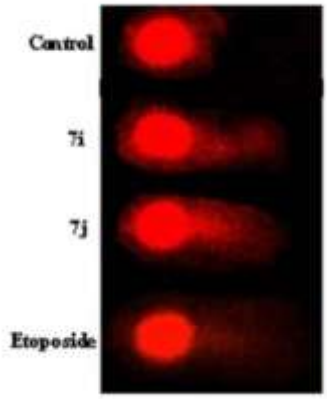

Figure 5: Comet assay showing the extent of DNA damage occurred with Podophyllotoxin linked β-carboline compounds are treated to DU-145 cells. Control; Podophyllotoxin linked β-carboline compound-1 (**7i**, 10 μM); Podophyllotoxin linked β-carboline compound -2 (**7j**, 10μM); Etoposide.

Cell cycle and apoptosis assay with β -carbolinebisindole compounds (**7g** and **7r**) at two different concentrations like 1μM and 2μM (to see dose effect on the cell cycle progressing and apoptosis). It was noticed that β -carbolinebisindole compounds stop cell cycle at G2/M phase and induce apoptosis in dose dependant manner. The results obtained are shown in figure 6 and 7.

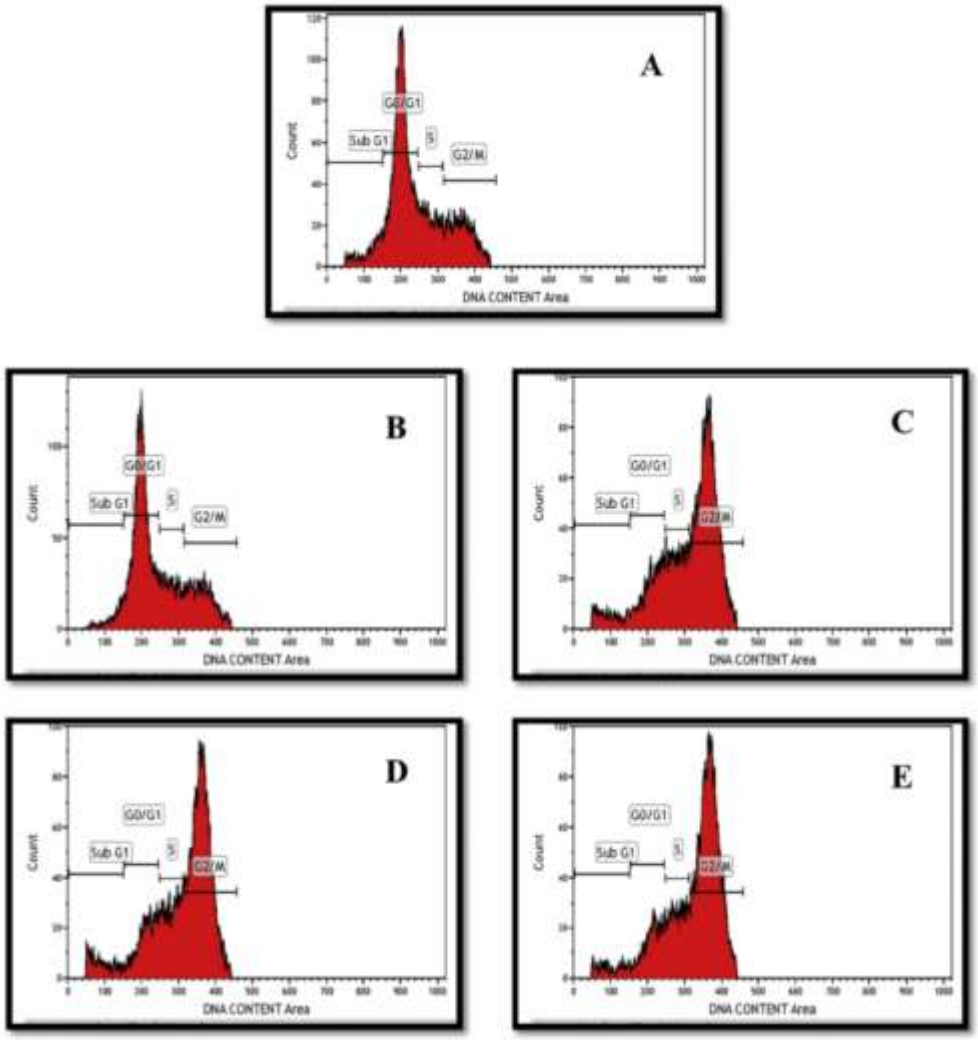

Figure 6: Flow cytometric analysis in DU-145 cells after treatment with two different β - carbolinebisindole compounds at 1 and 2 mM concentrations for 48 h. A: Control cells, B: β - carbolinebisindole compound, **7g** (1 mM), C: β -carbolinebisindole compound, **7g** (2 mM), D: β - carbolinebisindole compound-2, **7r** (1 mM) and E: β -carbolinebisindole compound- 2,**7r** (2 mM). Cell cycle inhibition at G2/M phase was noticed on addition of β - carbolinebisindole compounds.

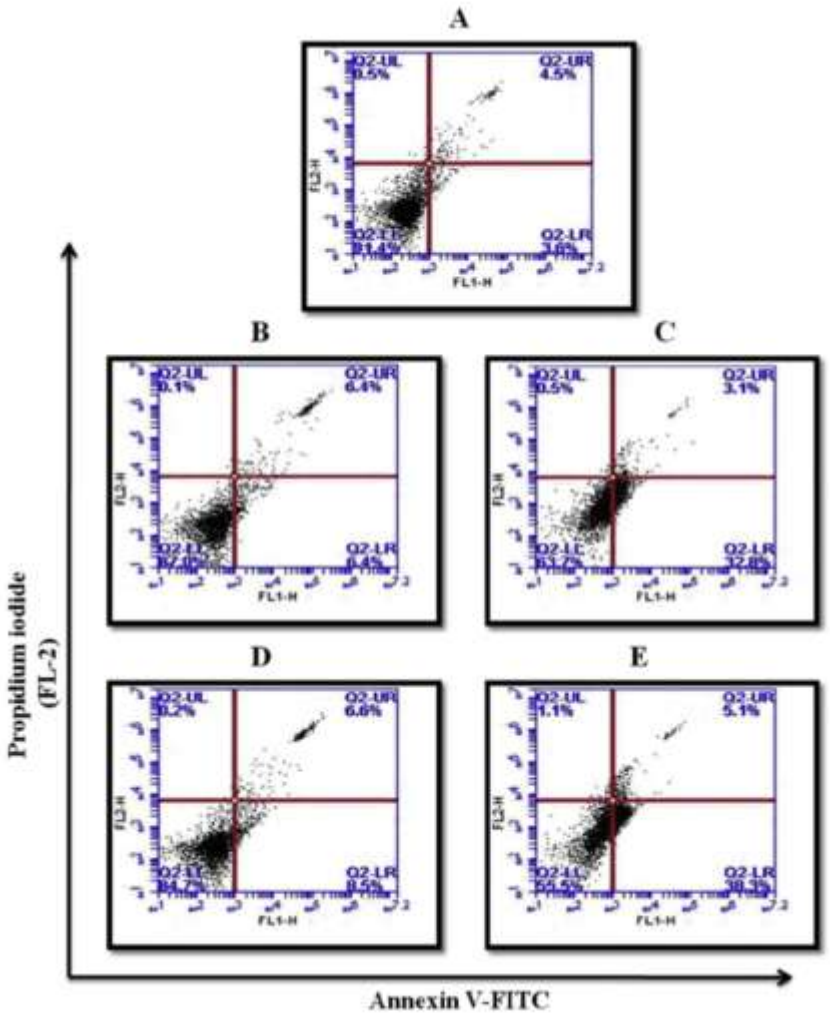

Figure 7: Annexin V-FITC/PI (AV/PI) dual staining assay: Quadrants; Upper left (necrotic cells), Lower left (live cells), Lower right (early apoptotic cells) and Upper right (late apoptotic cells). A: Control cells (DU-145), β -carbolinebisindole compound,**7g** (1 mM), C: β -carbolinebisindole compound,**7g** (2 mM), D: β -carbolinebisindole compound-2,**7r** (1 mM) and E: β –carboline bisindole compound-2,**7r** (2 mM).

The above mentioned studies with β-carboline linked molecules were carried out and the data obtained from these experiments were analysed and published in two international peer reviewed journals. The reference for each paper is provided below.

References of the papers in which the details of research was published:

1. Design, synthesis and biological evaluation of new b-carbolinebisindole compounds as DNA binding, photocleavage agents and topoisomerase I inhibitors. (2018) Jeshma Kovvuri , Burri Nagaraju, V. Lakshma Nayak, Ravikumar Akunuri, M.P. Narasimha Rao , Ayyappan Ajitha , Narayan Nagesh *, Ahmed Kamal *. European Journal of Medicinal Chemistry, 143, 1563-1577.(IF- 7).

2. Synthesis of podophyllotoxin linked β-carboline congeners as potential anticancer agents and DNA topoisomerase II inhibitors. (2018) M. Sathish, B. Kavitha, V.L. Nayak, Tangella Yellaiah , Ayyappan Ajitha, S. Nekkanti, A. Alarifi, N. Shankaraiah*, N. Nagesh*, Kamal A*. Eur J Med Chem.,144, 557-571. doi: 10.1016/j.ejmech.2017.12.055. (IF- 7).